Disagreement between theory and experiment grows with increasing rotational excitation of HD(v′, j′) product for the H + D2 reaction

Justin Jankunas, Mahima Sneha, Richard N. Zare, Foudhil Bouakline, and Stuart C. Althorpe

Citation: J. Chem. Phys. **138**, 094310 (2013); doi: 10.1063/1.4793557
View online: http://dx.doi.org/10.1063/1.4793557
View Table of Contents: http://jcp.aip.org/resource/1/JCPSA6/v138/i9
Published by the American Institute of Physics.

Disagreement between theory and experiment grows with increasing rotational excitation of HD(v', j') product for the H + D_2 reaction

Justin Jankunas,[1] Mahima Sneha,[1] Richard N. Zare,[1,a)] Foudhil Bouakline,[2] and Stuart C. Althorpe[3]
[1]*Department of Chemistry, Stanford University, Stanford, California 94305-5080, USA*
[2]*Max Born Institute, Max Born Strasse 2a, 12489 Berlin, Germany*
[3]*Department of Chemistry, University of Cambridge, Lensfield Road, Cambridge CB2 1EW, United Kingdom*

(Received 11 January 2013; accepted 13 February 2013; published online 5 March 2013)

The Photoloc technique has been employed to measure the state-resolved differential cross sections of the HD(v', j') product in the reaction H + D_2 over a wide range of collision energies and internal states. The experimental results were compared with fully dimensional, time-dependent quantum mechanical calculations on the refined Boothroyd-Keogh-Martin-Peterson potential energy surface. We find nearly perfect agreement between theory and experiment for HD(v', j') product states with low to medium rotational excitation, e.g., HD($v' = 1, j' = 3$) at a collision energy, E_{coll}, of 1.72 eV, HD($v' = 1, j' = 3, 5$) at $E_{coll} = 1.97$ eV, and HD($v' = 3, j' = 3$) at $E_{coll} = 1.97$ eV. As the rotational angular momentum, **j′**, of HD(v', j') increases, the agreement between theoretical predictions and experimental measurements worsens but not in a simple fashion. A moderate disagreement between theory and experiment has been found for HD($v' = 0, j' = 12$) at $E_{coll} = 1.76$ eV and increased monotonically for HD($v' = 0, j' = 13$) at $E_{coll} = 1.74$ eV, HD($v' = 0, j' = 14$) at $E_{coll} = 1.72$ eV, and HD($v' = 0, j' = 15$) at $E_{coll} = 1.70$ eV. Disagreement was not limited to vibrationless HD(v', j') product states: HD($v' = 1, j' = 12$) at $E_{coll} = 1.60$ eV and HD($v' = 3, j' = 8, 10$) at $E_{coll} = 1.97$ eV followed a similar trend. Theoretical calculations suggest more sideways/forward scattering than has been observed experimentally for high j' HD(v', j') states. The source of this discrepancy is presently unknown but might be the result of inaccuracy in the potential energy surface.
 [http://dx.doi.org/10.1063/1.4793557]

I. INTRODUCTION

Experimental and theoretical work on the H + H_2 reaction system and its isotopic cousins has been particularly fruitful in the last three decades or so.[1] With the use of laser techniques, experimental findings have been brought into close agreement with theory for both reactive[2–9] and inelastic[10,11] scattering, although some discrepancies seemed to remain.[12,13] It might be thought that theory is presently so well developed that the need to perform additional experiments has been removed. However, only recently have experiments led the way in understanding the dynamics of the reaction product when it is formed close to the limit of what energy can appear in internal excitation.[14,15] Once this behavior was found, it was seen to be present in the theoretical calculations as well. Even though theory and experiment showed the same trend, the agreement was qualitative rather than quantitative. The time has come to examine closely the agreement between theory and experiment, which is the topic of this paper for differential cross sections (DCS) in the reaction

$$H + D_2 \rightarrow HD(v', j') + D. \quad (1)$$

Let us concentrate on the DCS as a function of product rotational excitation. Generally, it was found that rotationally cold HD(v', j') products scatter backwards, while rotationally hot HD(v', j') molecules scatter into a more sideways/forward direction.[16–18] (Figure 1 is a cartoon depicting a collision between a hydrogen atom and a deuterium molecule; embedded are the definitions of backward and forward scattering to be used throughout this article.) The rationale for the observed behavior is completely classical. From the conservation of total angular momentum, low impact parameters between a hydrogen atom and a deuterium molecule result in rotationally cold HD(v', j') products, while collisions with nonzero orbital angular momentum are more effective at producing HD(v', j') with high **j′**.[19] As mentioned above, an exception occurs, resulting from the existence of a rotational barrier, when HD(v', j') is formed with high internal excitation.[14,15]

In this work, we focus on H + D_2 → HD(v', high j') + D collisions. Koszinowski *et al.*[20] studied the H + D_2 → HD($v' = 1, j' = 2, 6, 10$) + D reaction at several collision energies and reported a good overall agreement between theory and experiment, except for HD($v' = 1, j' = 10$) state at $E_{coll} = 1.84$ eV. They did not, "...find any obvious explanation for the deviating DCS measured for $j' = 10$ at $E_{coll} = 1.84$ eV."[20] Indeed, a closer examination of data in Bartlett *et al.*[21] hints at similar conclusions. DCS for HD($v' = 2, j' = 9$) at $E_{coll} = 1.61$ eV and $E_{coll} = 1.97$ eV show that theory predicts somewhat more sideways scattered products than what is measured experimentally.

a)Author to whom correspondence should be addressed. Electronic mail: zare@stanford.edu.

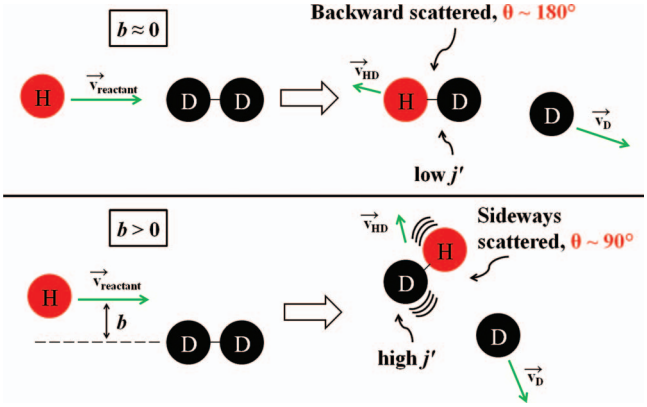

FIG. 1. Cartoon depicting head-on (upper panel) and glancing (lower panel) collisions between a hydrogen atom and a deuterium molecule. A low-impact-parameter collision leads to rotationally cold HD(v', j') products that are backward scattered, i.e., $\mathbf{v_{reactant}}$ and $\mathbf{v_{HD}}$ are antiparallel and θ is about 180°. Similarly, glancing collisions lead to rotationally excited products that are sideways/forward scattered. The forward direction corresponds to $\theta \sim 0°$, with $\mathbf{v_{reactant}}$ and $\mathbf{v_{HD}}$ being parallel (not shown), and a sideways direction is loosely defined as the $\theta \sim 90°$ scattering region, with $\mathbf{v_{reactant}}$ perpendicular to $\mathbf{v_{HD}}$.

We present a considerable amount of data in the form of state-to-state DCSs for the H + D_2 → HD(v', j') + D reaction at several E_{coll}. For some states, e.g., HD($v' = 3$, $j' = 10$) at $E_{coll} = 1.97$ eV, the disagreement between experiment and theory is striking. However, at low to moderate values of j', theory and experiment almost perfectly match. The remainder of the paper is organized as follows. Section II discusses the details of the experimental method; Sec. III outlines the theoretical methods employed in calculating the DCSs; Sec. IV contains the processed experimental data, which are compared to theory; Sec. V presents a discussion; and Sec. VI concludes the paper.

II. EXPERIMENTAL

The three-dimensional ion imaging instrument used in this study has been described in detail in previous publications.[21,22] Briefly, a 5% HBr in D_2 mixture was expanded supersonically through a pulsed nozzle (General Valve, Series 9) operating at 10 Hz, with a typical backing pressure of ~1300 Torr. A skimmed molecular beam (2 mm skimmer, Beam Dynamics) was intersected with a softly focused (60 cm lens) UV laser pulse polarized along the time-of-flight (TOF) axis. The UV laser pulse was generated by tripling the output of a dye laser (Lambda Physik, LPD 3000, operating on a DCM dye), pumped by the second harmonic of an Nd^{3+}:YAG laser (Spectra Physics, GCR Series). Sum-frequency mixing was accomplished with two BBO crystals. Pressure in the ionization and detection region was 1×10^{-8} Torr and 5×10^{-9} Torr with the nozzle off and ~2.5×10^{-7} Torr and ~1.4×10^{-7} Torr with the nozzle on, respectively.

In this study, we used only one laser beam. Our previous studies employed two lasers—one acting as a photolysis laser (to photodissociate the HBr molecule) and the other as a probe laser (to state-selectively ionize the HD(v', j') product). This was done mostly to keep the collision energy constant as the probe laser wavelength was scanned across different HD(v', j') resonance enhanced multiphoton ionization (REMPI) lines. Because a constant collision energy was not the main focus of this study, we decided to use only one laser to both photodissociate the HBr and detect the HD(v', j') products, all within the same ~8 ns laser pulse duration. This has also improved the overall signal-to-noise ratio. The HD(v', j') molecules were probed by means of [2+1] REMPI via the Q(j') branch members of the (0, v') vibrational band of the $E,F\ ^1\Sigma^+_g$–$X\ ^1\Sigma^+_g$ electronic transition. Each HD(v', j') REMPI line was scanned over its Doppler profile (±6 pm) because the HD(v', j') products had a substantial velocity, i.e., up to 10 000 m/s. The background subtraction was done by parking the laser off the REMPI line and scanning it for ±6 pm. All other experimental parameters, such as laser power and scan time, were kept constant for a particular HD(v', j') state when doing online and offline scans. HD^+ ions were collected using a time-of-flight mass spectrometer and detected by a position-sensitive delay line detector. The resultant three-dimensional HD(v', j') speed distributions with laser wavelength on and off the REMPI line were then subtracted to yield the true HD(v', j') reaction product speed distribution. All wavelengths were measured with a laser wavelength meter (Wavemaster, Coherent). Table I lists relevant experimental parameters used for the six HD(v', j') states studied.

III. THEORY

Fully quantum mechanical calculations of state-to-state DCSs were carried out using the wave packet method of Ref. 23. Quantum wave packets, containing a spread of desired collision energies, were propagated from the reactant (H + D_2) to the product (HD + D) asymptotic arrangements

TABLE I. Main experimental parameters for different HD(v', j') product states studied. Column 2 includes the zero point energy of HD(v', j') (0.23 eV). Column 3 lists the amount of internal energy of HD(v', j') as a fraction of total energy, defined as the sum of E_{coll}, the zero point energy of D_2 (0.19 eV), and the average rotational excitation of D_2 (0.023 eV). Column 8 gives the total number of ions collected after the background subtraction.

HD (v', j')	$E_{int}^{HD(v',j')}$, eV	$f_{HD(v',j')}$	E_{coll}, eV	REMPI (online) ± 6 pm, nm	REMPI (offline) ± 6 pm, nm	Laser power, μJ	Number of ions
$v' = 0, j' = 12$	1.02	0.52	1.76	207.520	207.556	650	5555
$v' = 0, j' = 13$	1.13	0.58	1.74	208.483	208.416	650	5344
$v' = 0, j' = 14$	1.25	0.65	1.72	209.501	209.561	1000	6406
$v' = 0, j' = 15$	1.38	0.72	1.70	210.574	210.605	900	4390
$v' = 1, j' = 3$	0.75	0.39	1.72	209.483	209.428	700	7704
$v' = 1, j' = 12$	1.43	0.79	1.60	214.993	215.040	780	3630

of the reaction, using the refined Boothroyd-Keogh-Martin-Peterson (BKMP2) potential energy surface.[24] The propagation of the wave packet was performed using the reactant-product decoupling method,[23] which decouples the nuclear motion into separate reactant, strong-interaction, and product regions, and allows different coordinates and basis sets to be used in each of these regions. Thus, the wave packet was represented on efficient basis sets constructed from grids based on (H + D_2) Jacobi coordinates in the reactant approach region, and (D + HD) coordinates in the strong-interaction and product exit regions.

A separate wave packet propagation was carried for each initial rotational quantum number j = 0,1,2 of the reactant D_2 molecule, and for each individual projection of j on the H + D_2 approach vector. The same calculations were repeated for all partial waves in the range J = 0–45, with the maximum projection of the total angular momentum on the intermolecular axis set to $\Omega = 30$. The parameters used in the calculations were sufficient to converge almost all the state-to-state cross sections to within better than 5%, over a continuous range of collision energies from 0.5 to 2.2 eV.

Given that the range of the collision energies considered here is well below the energy minimum of the conical intersection of the H_3 potential energy surface (PES), which occurs at 2.74 eV, coupling to the first excited state as well as the geometric phase effect, known to be negligible at these energies,[25] were excluded from our calculations.

IV. RESULTS

First, we show some of the raw data and how they are transformed to yield the DCSs. To facilitate the interpretation of figures that follow, we sketch in Fig. 2 the experimental apparatus with the affixed laboratory reference frame. The definition of laboratory axes should be particularly helpful in understanding three-dimensional ion images. The three velocity components, V_x, V_y, and V_z, of an HD^+ ion are measured as follows. Known voltages are applied in the z direction, which lies along the TOF axis (see Fig. 2). The arrival time of an ion yields the V_z component. No fields are present in x and y directions; hence, ions experience free motion in these two directions. A measurement of the ion's x and y positions on the

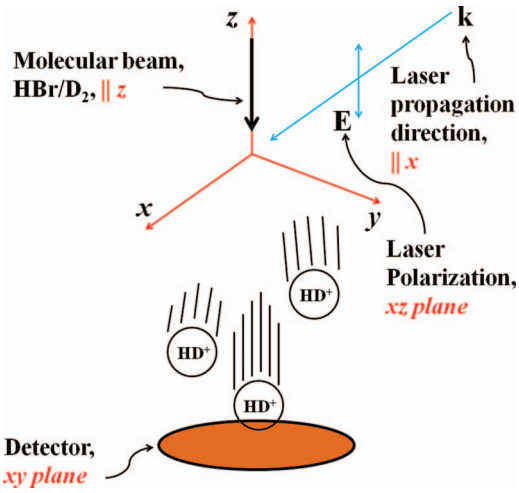

FIG. 2. Definition of the laboratory reference frame used in this study.

detector thus gives the V_x and V_y components. Figure 3 shows typical ion images. One can, in fact, infer some general features of the resulting DCS directly from these images. The radius of a sphere (or its projection) is directly proportional to an ion's speed. Given the allowed range of laboratory speeds, *vide infra*, one can deduce if the particular product in question is backward, sideways, or forward scattered. It is immediately evident that HD($v' = 0, j' = 14$) is sideways/forward scattered, based solely on the size of the image. This is particularly evident from Figs. 3(c)–3(e). Similarly, the ion sphere for HD($v' = 1, j' = 3$) is small (Figs. 3(g)–3(i)). This product is thus expected to be back scattered.

The resulting three-dimensional ion images are converted into a laboratory speed distribution via $V_{LAB}{}^2 = V_x{}^2 + V_y{}^2 + V_z{}^2$. Figure 4 shows two typical speed distributions. As expected, the HD($v' = 0, j' = 14$) speed distribution peaks at around 7000 m/s, closer to the maximum allowed speed, while the HD($v' = 1, j' = 3$) speed distribution peaks around 3500 m/s, closer to the minimum allowed speed (Figs. 4(a) and 4(b), respectively). Notice a peak at around 750 m/s in the case of HD($v' = 1, j' = 3$). This may arise from thermal HD in the molecular beam, although we have not spent too much effort trying to elucidate the origin of this peak, as it falls outside the Photoloc range and thus does not interfere with the speed inversion into the DCS.

In the Photoloc technique, the HD(v', j') laboratory speed distributions are converted to DCSs via the law of cosines.[26] The HD(v', j') speed distributions in the lab frame are obtained by subtracting the "offline," background, scan from the "online" scan (see the Experimental section for more details, as well as Fig. 4).

Figure 5 shows the DCSs for HD(v', low/medium j'). Because the agreement between theory and experiment for these states is nearly quantitative, there are no ambiguities, *vide infra*, in actually fitting the experimental data to absolute theoretical cross section calculations. Figure 5(a) contains the HD($v' = 1, j' = 3$) DCS at E_{coll} = 1.72 eV, which was measured under the conditions described in the Experimental section. Other measurements in Fig. 5 were made earlier,[14] using a dedicated photolysis laser and a separate probe laser. All these experiments were done at E_{coll} = 1.97 eV. Some of these data have been published by us in Ref. 13, and some have never been published before. The time-dependent quantum mechanical calculations (TD-QM) were blurred to account for the rotational distribution of the $D_2(v = 0, j = 0, 1$ and 2) reactant, the spread in the collision energies (0.05 eV) and the instrumental resolution (~500 m/s). The blurring protocol is analogous to that used in Refs. 14 and 21.

Often experimental and theoretical DCS are fitted simply by inspection.[20,21,27] This is because molecular experiments measure relative and not absolute cross sections. One is free to multiply the experimental results by the same common factor F to fit the theory. To judge the degree of agreement more quantitatively, it is natural to introduce a least squares fitting procedure. We use the familiar formulas

$$S = \sum_{i=1}^{i=N} (I(\theta_i)^{\text{theory}} - F \cdot I(\theta_i)^{\text{experiment}})^2, \qquad (2)$$

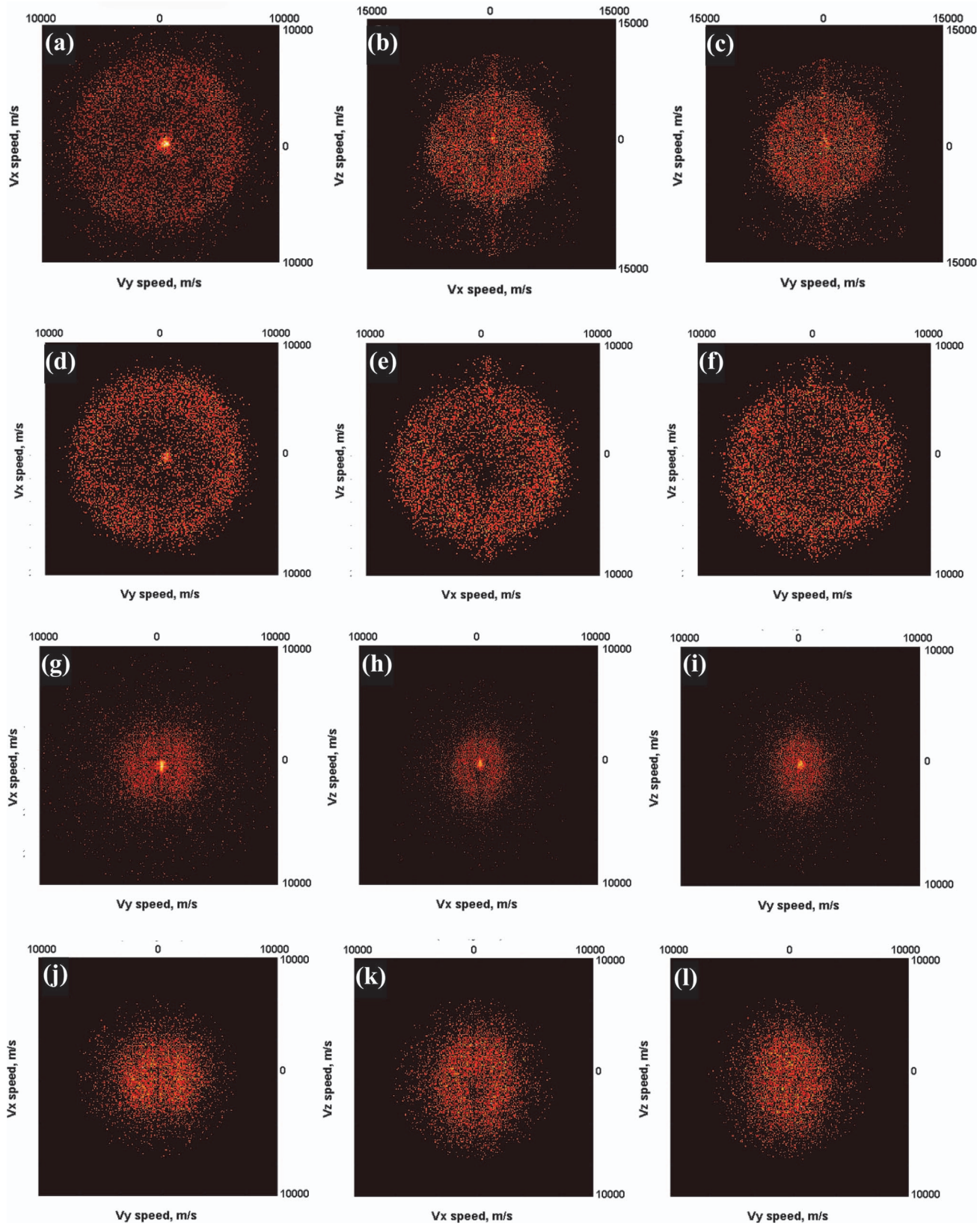

FIG. 3. Representative ion images (a)–(f) for HD($v' = 0, j' = 14$) at $E_{coll} = 1.72$ eV, and (g)–(l), for HD($v' = 1, j' = 3$) at $E_{coll} = 1.72$ eV. All images are projections of a three-dimensional ion sphere along the specified directions. Panels (a) through (c) are raw, unprocessed ion images for HD($v' = 0, j' = 14$). The intense feature in the middle of (a) corresponds to a molecular beam background, centered at around $V_x \approx V_y \approx 0$ m/s. This background is also evident in V_x/V_z and V_y/V_z projections, (b) and (c), respectively. Note also the expanded scale in (b) and (c), which facilitates seeing that the molecular beam background strikes the detector at all times. Rejection of the slow-moving molecular beam background results in much more revealing images, shown in (d) through (f). A trained eye could even infer the nature of the DCS: high measured speeds correspond to sideways/forward scattered HD($v' = 0, j' = 14$). Unprocessed images (g) through (i), corresponding to rotationally cold HD($v' = 1, j' = 3$), immediately suggest that this molecular product has smaller lab speeds, and is backscattered. Note also that the molecular beam background in this case is very different from the one shown in (b) and (c)—it only occupies the center of the sphere. Panels (j) through (l) show the resulting ion images with background at the center removed.

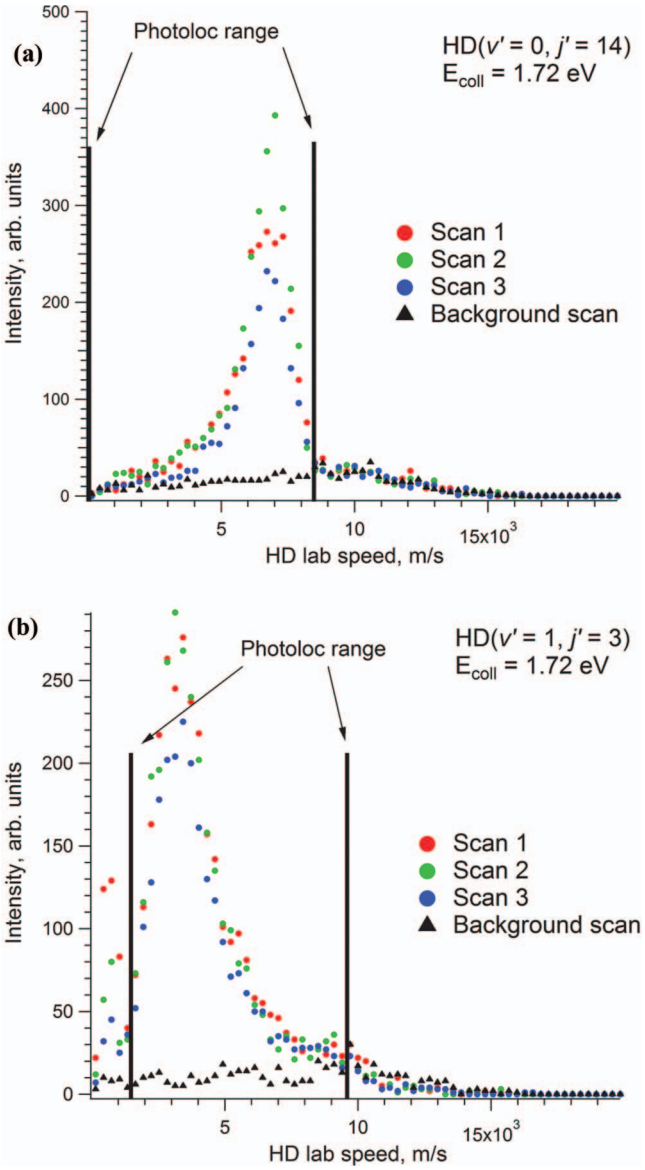

FIG. 4. Laboratory speed distributions for (a) HD($v' = 0, j' = 14$) and (b) HD($v' = 1, j' = 3$). Note a substantial molecular beam background in the case of HD($v' = 1, j' = 3$) product at $v_{LAB} \approx 750$ m/s, that, fortuitously, is outside the Photoloc range and hence does not interfere with the DCS measurement.

where $I(\theta_i)^{\text{theory}}$ and $I(\theta_i)^{\text{experiment}}$ are the theoretical and experimental values of DCS at a particular angle θ_i, respectively, and N is the number of data points and ranges typically between 20 and 35 in this experiment. The best F value in a least squares sense is found from

$$\frac{\partial S}{\partial F} = \sum_{i=1}^{i=N} I(\theta_i)^{\text{experiment}} I(\theta_i)^{\text{theory}} - F \cdot (I(\theta_i)^{\text{experiment}})^2 = 0. \tag{3}$$

We characterize the fit by introducing the familiar R^2 parameter:[28]

$$R^2 \equiv 1 - \frac{\sum_{i=1}^{i=N} (I(\theta_i)^{\text{theory}} - F_{best} \cdot I(\theta_i)^{\text{experiment}})^2}{\sum_{i=1}^{i=N} (I(\theta_i)^{\text{experiment}})^2}, \tag{4}$$

where F_{best} is the optimum value found from Eq. (3). The R^2 value indicates the overall quality of the fit between experiment and theory, where $R^2 = 1$ indicates a perfect fit whereas $R^2 = 0$ suggests a very poor fit. Table II presents R^2 values for the data shown in Fig. 5. Clearly, all the fits are extremely good—the R^2 values for five states are $R^2 > 0.96$. The agreement between experiment and theory is somewhat worse for HD($v' = 3, j' = 5$) with $R^2 = 0.941$. Relative uncertainties in the fit parameter F are small (see Table II).

TABLE II. R^2 values for the least-squares fit of experiment to theory for HD(v', j') states shown in Fig. 5. Also tabulated are relative uncertainties in the fit parameter F.

HD(v', j') state	R^2	$\delta F/F$,%
$v' = 1, j' = 3$ (Fig. 5(a))	0.973	3.1
$v' = 1, j' = 2$ (Fig. 5(b))	0.985	2.7
$v' = 1, j' = 3$ (Fig. 5(c))	0.982	2.3
$v' = 1, j' = 5$ (Fig. 5(d))	0.971	2.9
$v' = 3, j' = 3$ (Fig. 5(e))	0.982	2.4
$v' = 3, j' = 4$ (Fig. 5(f))	0.966	3.4
$v' = 3, j' = 5$ (Fig. 5(g))	0.941	4.7

The DCSs for HD(v', high j') are shown in Fig. 6. The DCSs in Figs. 6(b)–6(f) were obtained under the experimental conditions described above, whereas, the DCSs in Figs. 6(a) and 6(g), and 6(h) were obtained at $E_{coll} = 1.97$ eV under two-laser conditions (see Ref. 14). The fitting of experimental data to theoretical calculations in this case is less straightforward than the DCS for HD(v', low/medium j') in Fig. 5. One can, of course, minimize the sum in Eq. (2) to find the optimum fit in a least squares sense. We find that although such fits are mathematically the best, from a physical point of view one could also have other fits with lower R^2 values. One of the most naïve approaches for fitting the experiment to theory would be to maximize the number of data points that coincide within the experimental uncertainty. Another approach is to fit the experiment to theory by matching their peak heights. We have used the latter strategy in the past, for example, by fitting the data for HD($v' = 2, j'$).[21] In summary, there are three ways one could go about fitting the experimental and theoretical data: (1) a fit that maximizes the R^2 value, which we call "fit 1," (2) a fit that has the greatest number of experimental and theoretical points coinciding (within the experimental uncertainty), "fit 2," and (3) a fit that matches the experimental and theoretical peak heights, "fit 3." We found that "fit 1" is usually a compromise between "fit 2" and "fit 3." We therefore do not include "fit 1" in Fig. 6 to avoid clutter. Instead, we present "fit 2" (blue triangles) and "fit 3" (red circles). We tabulate relevant R^2 values for HD(v', high j') states in Table III.

V. DISCUSSION

The most striking feature of DCS that emerges after examining Figs. 5 and 6 is the fact that as the rotational angular momentum of the HD(v', j') product increases, the agreement between theory and experiment worsens.[29] Determining which fit is the "correct" one, i.e., "fit 1" vs. "fit 2" vs. "fit 3," in the case of HD(v', high j') DCS, Fig. 6, is nontrivial. For example, from a purely mathematical point of view

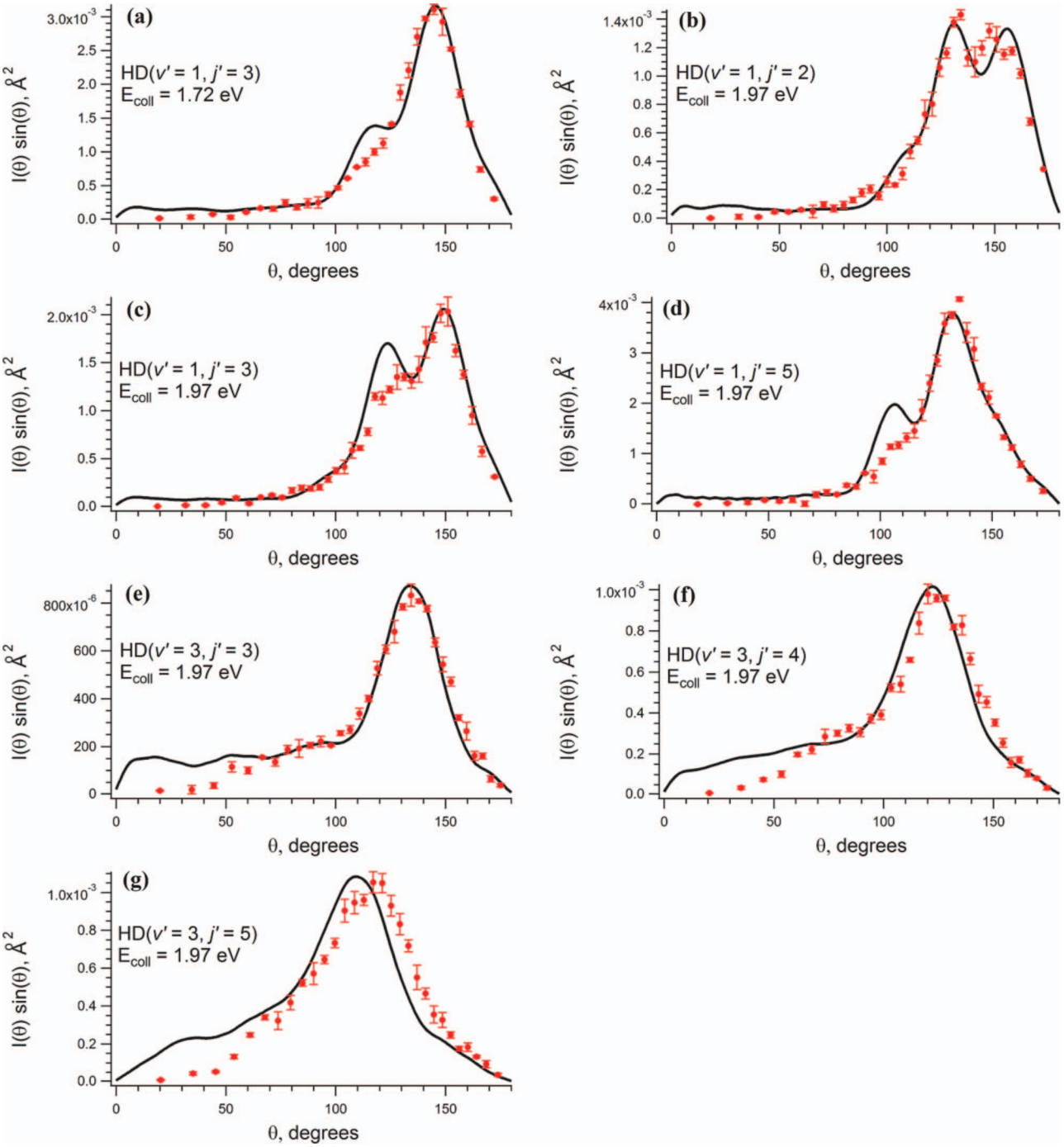

FIG. 5. DCS for the HD(v', j') product of the H + D_2 → HD(v', j') + D reaction. Red dots are the experimental data; the error bars correspond to one standard deviation of three to five independent measurements. The fit represents the least squares fit, with associated R^2 values (Table II). Black curve is the blurred TD-QM calculations.

"fit 1" should be used. Indeed, if the theoretical calculations were known to be 100% correct, then "fit 1" would make the most sense. The purpose of this study, however, is twofold. Not only is experiment compared to theory; theory is also compared to experiment. Following this line of logic, one inevitably arrives at the dilemma, "Which curve should be trusted more—the theoretical or the experimental one?" Let us imagine that the experimental measurement is 100% correct. It would seem that in this case "fit 2" should be used as it correctly captures the largest portion of a theoretical curve. The worst case scenario is the one in which theory and experiment are both inaccurate. It is not obvious then which fit is most appropriate.

From an experimental point of view, the best one can do is to eliminate as many systematic errors as possible. Because the DCSs are obtained from the measured speed distributions, the most obvious place to start is by discussing the accuracy of a speed measurement in the laboratory reference frame. We performed several tests toward this end. We have, for example, measured the H-atom speed following the

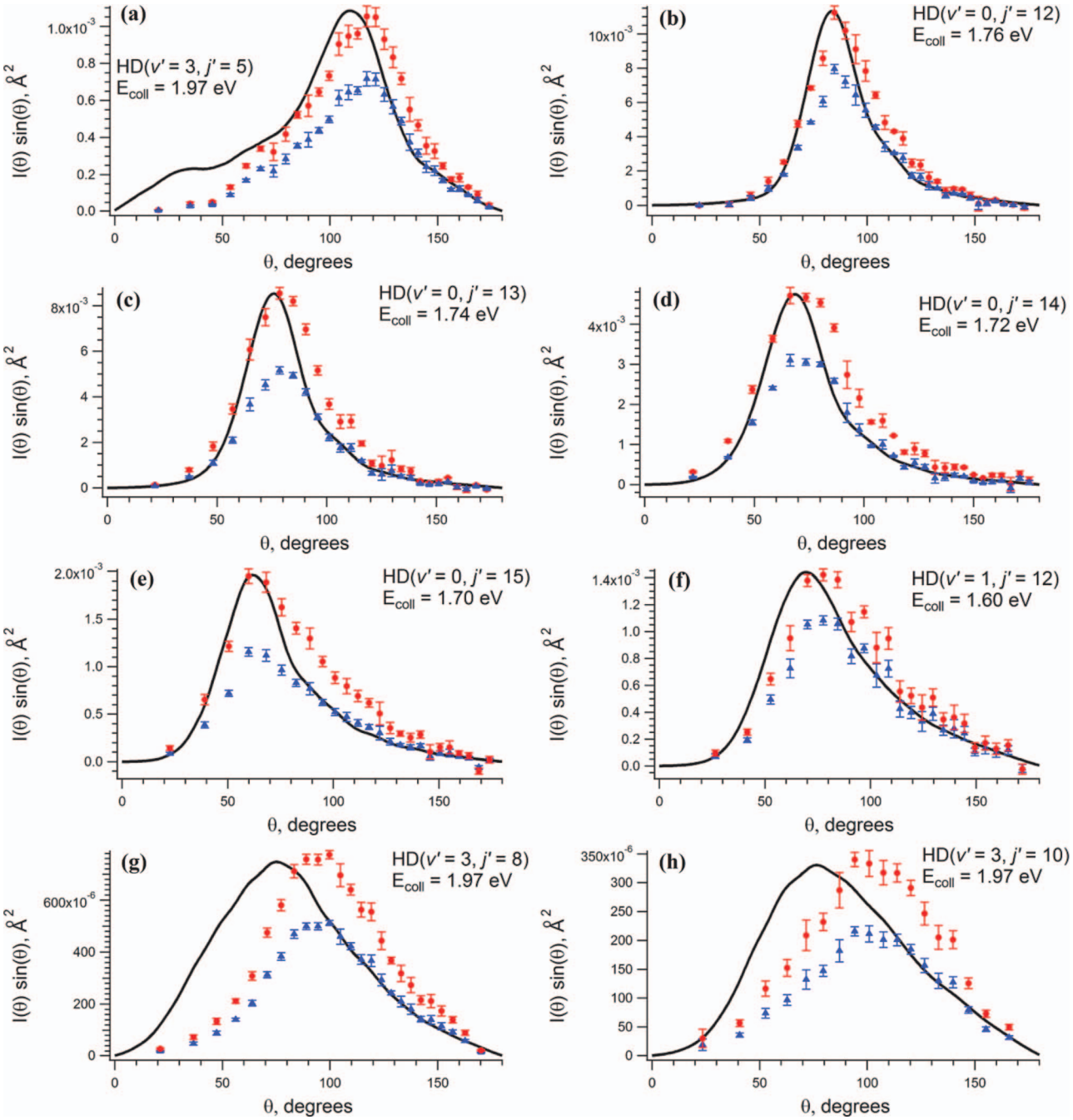

FIG. 6. DCS for the HD(v', j') product of the H + D_2 → HD(v', j') + D reaction. Circles and triangles are the experimental data; the error bars correspond to one standard deviation of three to five independent measurements. Red circles are a fit of an experimental data to theory wherein the peak heights are matched, "fit 3." Blue triangles are a fit wherein the number of experimental and theoretical points that coincide (within the experimental error) is maximum, "fit 2." Black curve is the blurred TD-QM calculations.

photodissociation of an HBr molecule, i.e.,

$$\mathrm{HBr} + h\upsilon \rightarrow \mathrm{H} + \mathrm{Br/Br^*}, \tag{5}$$

where Br* denotes a spin-orbit-excited bromine atom. The H atom was probed by means of a [2+1] REMPI via its 2*s* state at 243.068 nm. The measured H-atom speeds were within 100 m/s of the calculated ones. (The absolute H-atom speeds in this case are large; up to 20 000 m/s; a mere 0.5% error.)

However, a more convincing argument for the absence of systematic errors in the laboratory speed measurement comes from the examination of speed distributions for several HD(v', j') states; see Table IV. From Figs. 6(g) and 6(h), it is evident that there is a substantial disagreement between experiment and theory for HD($v' = 3$, $j' = 8$ and 10), respectively. From Table IV, we see that in the case of HD($v' = 3$, $j' = 10$) the peak in the measured speed distribution is ∼4500 m/s. If indeed there were any systematic errors in measuring laboratory speeds around 4500 m/s, or molecules were being underdetected at 4500 m/s, this would mean that other HD(v', j') states with similar speed peaks should exhibit deviations from theory. HD($v' = 1$, $j' = 5$), for example, has a peak in its speed distribution at ∼4150 m/s—a value that is very close to the

TABLE III. R^2 values for "fit 1," "fit 2," and "fit 3" (see text for details) for HD(v', j') states shown in Fig. 6.

HD(v', j') state	R^2, "fit 1"	R^2, "fit 2"	R^2, "fit 3"
$v' = 3, j' = 5$ (Fig. 6(a))	0.941	0.703	0.938
$v' = 0, j' = 12$ (Fig. 6(b))	0.959	0.838	0.958
$v' = 0, j' = 13$ (Fig. 6(c))	0.957	0.766	0.942
$v' = 0, j' = 14$ (Fig. 6(d))	0.953	0.825	0.930
$v' = 0, j' = 15$ (Fig. 6(e))	0.941	0.732	0.926
$v' = 1, j' = 12$ (Fig. 6(f))	0.939	0.880	0.938
$v' = 3, j' = 8$ (Fig. 6(g))	0.814	0.520	0.812
$v' = 3, j' = 10$ (Fig. 6(h))	0.858	0.541	0.858

4500 m/s observed for HD($v' = 3, j' = 10$)—yet the DCS for HD($v' = 1, j' = 5$) is in a very good agreement with theory, as can be seen from Fig. 5(d). Similarly, the second peak in the speed distribution of the HD($v' = 1, j' = 2$) product is centered around 4400 m/s—even closer to the 4500 m/s of HD($v' = 3, j' = 10$)—yet the match to theory is almost perfect. Although the above argument does not rule out the possibility of a systematic error in our experiments, presently we cannot identify the source of such an error. In addition, we find no correlation of disagreement with the size of the absolute reaction cross section, so it is not a matter that weaker signals cause larger deviations from theory.

We have also considered a possible contribution to the signal from the slower-moving H atoms corresponding to Br* production in Eq. (5). To begin with, HD($v' = 3, j' = 8$ and 10) states cannot in principle be populated by the slower-moving H atom as these hydrogen atoms lack the kinetic energy required to produce these highly internally excited states. In addition, the "... long-standing problem concerning the relative contributions from the slow and fast channels..." has been solved by Koszinowski *et al.*[20] They find that, "...the magnitude of the correction term is largest for low j' states..."[20] Indeed, they find a negligible contribution from the slower-moving H atoms in the H + D_2 → HD($v' = 1, j' = 6$ and 10) + D reaction channels. We therefore assume that the slow-channel contribution to HD($v' = 0, j' = 12$–15) highly rotationally excited states is also minimal and cannot account for the disagreement.

TABLE IV. The allowed (Photoloc) speed range for a particular HD(v', j') state (column 3) and the maximum in the experimentally measured speed distribution (column 4).

HD(v', j')	E_{coll}, eV	Allowed lab speed range, m/s	Observed lab speed maximum, m/s
$v' = 0, j' = 12$	1.76	836–9060	6700
$v' = 0, j' = 13$	1.74	494–8667	6700
$v' = 0, j' = 14$	1.72	104–8223	6700
$v' = 0, j' = 15$	1.70	344–7719	6700
$v' = 1, j' = 3$	1.72	1445–9565	3400
$v' = 1, j' = 12$	1.60	786–7047	5500
$v' = 1, j' = 2$	1.97	1774–10457	3000 and 4400 (two peaks)
$v' = 1, j' = 3$	1.97	1709–10391	3400
$v' = 1, j' = 5$	1.97	1509–10192	4150
$v' = 3, j' = 3$	1.97	393–8289	3250
$v' = 3, j' = 4$	1.97	517–8165	4100
$v' = 3, j' = 5$	1.97	675–8007	4300
$v' = 3, j' = 8$	1.97	1401–7282	5200
$v' = 3, j' = 10$	1.97	2206–6477	4500

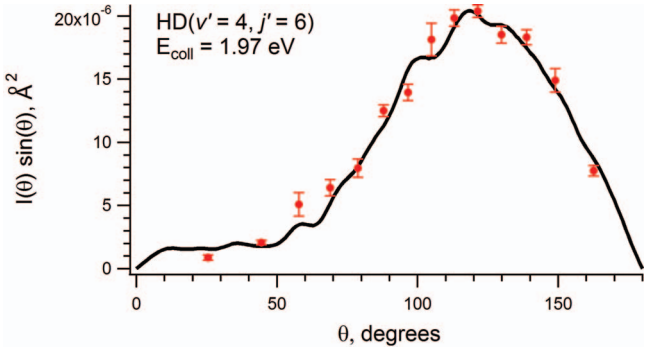

FIG. 7. DCS for the HD(v', j') product of the H + D_2 → HD($v' = 4, j' = 6$) + D reaction. Red dots are the experimental data; the error bars correspond to one standard deviation of four independent measurements. Black curve is the blurred TD-QM calculations.

In order to proceed further, i.e., in discussing the discrepancies between the experiment and theory, one needs to decide which fit is the "right" one, *vide supra*. We choose "fit 2," blue triangles in Fig. 6, the fit that maximizes the number of experimental and theoretical points that coincide (within the experimental uncertainty). We shall discuss the implications of using "fit 3" later.

It should be pointed out, that for the most part the agreement between experiment and theory is nearly quantitative, as shown in Fig. 5. For example, the experimental DCS of the HD($v' = 1, j' = 2$) state ($R^2 = 0.985$) is actually able to resolve two theoretically predicted peaks, Fig. 5(b), even if the experiment seems to under-estimate this second peak in the HD($v' = 1, j'$) manifold as j' increases from $j' = 2$, to $j' = 3$ ($R^2 = 0.982$) and to $j' = 5$ ($R^2 = 0.971$), Figs. 5(b) through 5(d), respectively. Close examination of the experimental data does show more than one peak but much less pronounced than theoretically predicted. Greaves *et al.*[30] found theoretically multiple indirect mechanisms in the DCS for H + D_2 → HD($v' = 0, j' = 0$) + D reaction, which are largely influenced by the conical intersection. The multiple peaks in our data for HD($v' = 1, j'$) may be the consequence of similar interactions with the conical intersection. It has been also suggested that the second peak may be a consequence of an interference between the direct recoil mechanism and an indirect one which arises from interactions with the conical intersection.[20] Presently, however, we do not know the origin of why the experimental data underestimate the smaller peak.

Similarly, HD($v' = 3, j' = 3$ and 4) states demonstrate a very good agreement between theory and experiment, $R^2 = 0.982$ and 0.966, respectively. In this case, the experiment under-estimates the amount of forward-scattered molecules at angles smaller than ~50°. We also point out that for the DCSs in Figs. 5(a)–5(f) the three different fits discussed above are basically indistinguishable from each other. In other words, the fit shown has the highest R^2 value, matches the main peak and has the maximum number of matching points (within the experimental error). In Fig. 5, HD($v' = 3, j' = 5$) is the only state where differences between experiment and theory

become noticeable, resulting in the smallest $R^2 = 0.941$. (We show the least-squares fit, "fit 1," for this state in Fig. 5(g) and then "fit 2" and "fit 3" in Fig. 6(a)).

The disagreement seems modest for the HD($v' = 0$, $j' = 12$) state, but increases substantially for the HD($v' = 0$, $j' = 15$) product, Fig. 6(b) and 6(e), respectively. Table III shows the R^2 values for these HD(v', high j') states. Firstly, "fit 1" has smaller R^2 values for HD(v', high j') states (column 2, Table III) than the corresponding R^2 values for HD(v', low/medium j') products (column 2, Table II). Secondly, "fit 1" R^2 values for HD(v', high j') states seem to decrease monotonically in going from HD($v' = 0$, $j' = 12$) to HD($v' = 0$, $j' = 15$). This is evidenced by a visual inspection of the DCSs in Figs. 6(b)–6(e). Interestingly, "fit 2" R^2 values decrease in a non-monotonic fashion (column 3, Table III) in going from HD($v' = 0$, $j' = 12$) to HD($v' = 0$, $j' = 15$). This is not too surprising, because "fit 2" is just a forced fit to maximize the number of experimental and theoretical points that coincide (blue triangles in Fig. 6). Similar disagreement between theory and experiment is observed for HD($v' = 1$, $j' = 12$). The more vibrationally excited HD($v' = 3$, j') manifold exhibits noticeable deviations between experiment and theory even for HD($v' = 3$, $j' = 5$), Fig. 6(a). HD($v' = 3$, $j' = 8$ and 10) states are examples of even larger discrepancies between experiment and theory, Figs. 6(g) and 6(h), respectively. One common feature emerges from looking at "fit 2" in all the DCSs in Fig. 6—it seems from this fitting choice that theory overestimates the amount of forward scattered HD(v', j') product.

At first, it might seem that the disagreement is just a matter of rotational excitation of the product, but more examination shows that the dependence on the product rotational quantum number j' is not so straightforward. Figure 7 shows the DCS for HD($v' = 4$, $j' = 6$). In this case, the agreement is startlingly close. Compare this with less rotationally excited HD($v' = 3$, $j' = 5$) product, shown in Fig. 6(a). How can we reconcile these disparate behaviors? We suggest that the nature of the disagreement is actually related to the impact parameter. As discussed previously, the HD($v' = 4$, $j' = 6$) product is formed very close to the energetic threshold, causing smaller impact parameters to contribute more than larger ones because of the centrifugal barrier in the exit channel.[14,15] Compare also the disagreement in HD($v' = 0$, j') to that in the HD($v' = 3$, j') states. For the former, the disagreement only becomes apparent at $j' = 12$ whereas for the latter the disagreement appears for $j' = 5$. Again, a simple argument about the magnitude of the product rotational excitation is inadequate. Previously, we found that high vibrational excitation for the inelastic H + D_2 scattering process arises from a "tug-of-war" in which the incoming H atom at large impact parameters pulls on the closest D atom before the H atom escapes in a frustrated chemical reaction.[31,32] We suggest that large impact parameters are also more efficient in producing vibrationally excited reactive scattering products. This reasoning then suggests to us that the disagreement between theory and experiment worsens with increasing impact parameter.

There are two possible sources of error in the theoretical calculations—errors in the potential energy surface (PES), and errors in the quantum dynamics calculations, which use the PES to compute the experimental observables. We are reasonably confident that dynamics errors can be ruled out, since the calculations were repeated twice, using time-dependent wave packet and time-independent (ABC[33]) methods, which gave DCSs in very close agreement for all values of j'. Any errors in the theoretical results are thus more likely to result from defects in the BKMP2 PES. This is in general an excellent PES (as the near-quantitative agreement of the majority of j' products testifies). However, the BKMP2 PES is known to contain errors in the long-range anisotropy, and it is conceivable that these could preferentially affect the scattering into the HD(v', high j') products. For example, it might be that the small van der Waals wells in the H_3 potential affect the mixing of the HD(v', high j') rotational states (since these have the least translational energy), or they might influence the high impact-parameter collisions, which lead preferentially to sideways scattered HD(v', high j') products.

In addition, the degree of disagreement between theory and experiment is v' dependent, Fig. 6. HD($v' = 0$, $j' = 12$–15) states, Figs. 6(b)–6(e), exhibit substantial disagreement at the peak of the DCS, however show improved agreement in the forward tail of the DCS. HD($v' = 3$, $j' = 5$, 8 and 10) states, Figs. 6(a), 6(g), and 6(h), respectively, behave differently: there is a good agreement only in the backward direction; sideways and forward directions are overestimated by theory.

Very similar behavior has been found for the H + D_2 → HD($v' = 1$, $j' = 10$) reaction at 1.72 eV ≤ E_{coll} ≤ 1.94 eV.[20] The HD($v' = 1$, $j' = 10$) theoretically predicted DCS is more sideways/forward scattered than the experimental measurement. Similar behavior has been found for the H + D_2 → HD($v' = 2$, $j' = 9$) reaction at E_{coll} = 1.97 eV—experimentally measured DCS are always more backward scattered than predicted theoretically.[21] We are therefore eager to learn if others have observed a similar disagreement between theory and experiment. Unfortunately, we were not able to find a joint experimental-theoretical DCS study that examined any isotopic variant of the H + H_2 reaction with the state-specific detection of H_2(v', high j'), HD(v', high j'), or D_2(v', high j'). Welge and co-workers,[17] for example, studied the H + D_2 → HD(v', j') + D reaction at E_{coll} = 1.28 eV. The highest j' states they looked at were HD($v' = 0$, $j' = 11$), HD($v' = 1$, $j' = 11$), and HD($v' = 2$, $j' = 7$). High j' DCSs shown in Fig. 13 of Ref. 17 are very hard to read because these small-cross section states were plotted together with higher-cross section low j' states. It appears, however, that the HD($v' = 0$, $j' = 11$) DCS agrees well with QM calculations. HD($v' = 1$, $j' = 9$) state, for example, seems to exhibit some discrepancies, however, it is difficult to draw any more concrete conclusions owing to the extremely fine scale of the graph. It is impossible to comment on the quality of the HD($v' = 1$, $j' = 10$ and 11) fits. The HD($v' = 2$, $j' = 6$) DCS shows considerable disagreement between theory and experiment. In another study by Welge and co-workers[34] at higher collision energy (2.20 eV), experiment and theory appear to agree closely, although the experimenters were not able to measure the very forward direction of HD product scattering.

The above discussion pertains to "fit 2" in Fig. 6. Clearly, very different conclusions would be reached in the case of "fit 3" in Fig. 6. For the HD($v' = 0$, $j' = 12$–15) product channels, Figs. 6(b)–6(e), it is the more backward direction of the DCS that is being underestimated theoretically. One would therefore think that lower-impact parameters are more effective at producing HD($v' = 0$, $j' = 12$–15) products than predicted theoretically—a radically different conclusion from the one reached when discussing "fit 2," where the importance of high-impact parameters was overestimated. This is the biggest drawback of any experimental method that measures relative cross sections as opposed to the absolute ones.

VI. CONCLUSIONS

We find evidence for a growing disagreement between the differential cross sections found from QM calculations and experimental measurements for the $H + D_2 \rightarrow HD(v', j') + D$ as j' increases. A more careful analysis shows that the disagreement between theory and experiment is more closely linked with increasing impact parameter, *vide supra*. These conclusions are further supported by the work of Koszinowski *et al.*[20] and Bartlett *et al.*[21] On the other hand, the work by Welge and co-workers[17,34] does not support our findings, at least in some instances, although it should be pointed out that their experiment did not measure the very forward region of the DCS.[34] The disagreement is large enough, particularly for HD($v' = 0$, $j' = 15$) and HD($v' = 3$, $j' = 8$, 10) states, that even the fitting procedure is not straightforward. If the experimental data are fitted to theory by making sure that as many experimental and theoretical points coincide, one arrives at a conclusion that presently the BKMP2 surface overestimates the reactivity of high-impact-parameter collisions between a hydrogen atom and a deuterium molecule leading to highly rotationally excited HD(v', j') products. We also find evidence that the disagreement between theory and experiment is sensitive to the vibrational excitation of the HD(v', j') diatomic. For HD products in their ground vibrational state, the disagreement is modest for HD($v' = 0$, $j' = 12$) state but is substantial for HD($v' = 0$, $j' = 15$). The $v' = 3$ vibrational manifold has noticeable disagreement between theory and experiment for j' values as low as $j' = 5$. In the present study, HD($v' = 3$, $j' = 8$ and 10) states have the lowest degree of agreement between theory and experiment. Together with the DCS for HD($v' = 4$, $j' = 6$) product, shown in Fig. 7, we believe that it is the impact parameter that is better correlated to the disagreement between theory and experiment than the j' value of HD diatomic product. Currently, the source of this disagreement has not been established. It may arise from an unrecognized systematic error in the experimental measurements, or from errors in the theoretical calculations, most probably in the BKMP2 potential energy surface.

ACKNOWLEDGMENTS

J.J., M.S., and R.N.Z. thank the US National Science Foundation for support of this work (NSF CHE Nos. 1025960 and 1151428). S.C.A. acknowledges support from the UK Engineering and Physical Sciences Research Council.

[1] F. J. Aoiz, L. Banares, and V. J. Herrero, Int. Rev. Phys. Chem. **24**, 119 (2005), and references therein.
[2] E. E. Marinero, C. T. Rettner, and R. N. Zare, J. Chem. Phys. **80**, 4142 (1984).
[3] J. J. Valentini and D. P. Gerrity, Int. J. Chem. Kinet. **18**, 937 (1986).
[4] K.-D. Rinnen, D. A. V. Kliner, R. S. Blake, and R. N. Zare, Chem. Phys. Lett. **153**, 371 (1988).
[5] D. A. V. Kliner, K-D. Rinnen, and R. N. Zare, Chem. Phys. Lett. **166**, 107 (1990).
[6] D. A. V. Kliner, D. E. Adelman, and R. N. Zare, J. Chem. Phys. **94**, 1069 (1991).
[7] D. Neuhauser, R. S. Judson, D. J. Kouri, D. E. Adelman, N. E. Shafer, D. A. V. Kliner, and R. N. Zare, Science **257**, 519 (1992).
[8] B. D. Bean, F. Fernandez-Alonso, and R. N. Zare, J. Phys. Chem. A **105**, 2228 (2001).
[9] F. Ausfelder, A. E. Pomerantz, R. N. Zare, S. C. Althorpe, F. J. Aoiz, L. Banares, and J. F. Castillo, J. Chem. Phys. **120**, 3255 (2004).
[10] A. E. Pomerantz, F. Ausfelder, R. N. Zare, J. C. Juanes-Marcos, S. C. Althorpe, V. S. Rabanos, F. J. Aoiz, L. Banares, and J. F. Castillo, J. Chem. Phys. **121**, 6587 (2004).
[11] P. G. Jambrina, J. Aldegunde, J. F. Castillo, F. J. Aoiz, and V. S. Rabanos, J. Chem. Phys. **130**, 031102 (2009).
[12] A. E. Pomerantz, F. Ausfelder, R. N. Zare, S. C. Althorpe, F. J. Aoiz, L. Banares, and J. F. Castillo, J. Chem. Phys. **120**, 3244 (2004).
[13] R. N. Zare, Annu. Rev. Phys. Chem. **64**, 1 (2013).
[14] J. Jankunas, R. N. Zare, F. Bouakline, S. C. Althorpe, D. Herraez-Aguilar, and F. J. Aoiz, Science **336**, 1687 (2012).
[15] J. Aldegunde, D. Herráez-Aguilar, P. G. Jambrina, F. J. Aoiz, J. Jankunas, and R. N. Zare, J. Phys. Chem. Lett. **3**, 2959 (2012).
[16] S. D. Chao, S. A. Harich, D. X. Dai, C. C. Wang, X. Yang, and R. T. Skodje, J. Chem. Phys. **117**, 8341 (2002).
[17] L. Schnieder, K. Seekamp-Rahn, E. Wrede, and K. H. Welge, J. Chem. Phys. **107**, 6175 (1997).
[18] B. D. Bean, J. D. Ayers, F. Fernandez-Alonso, and R. N. Zare, J. Chem. Phys. **116**, 6634 (2002).
[19] R. D. Levine and R. B. Bernstein, *Molecular Reaction Dynamics and Chemical Reactivity* (Oxford University Press, New York, 1987).
[20] K. Koszinowski, N. T. Goldberg, J. Zhang, R. N. Zare, F. Bouakline, and S. C. Althorpe, J. Chem. Phys. **127**, 124315 (2007).
[21] N. C.-M. Bartlett, J. Jankunas, T. Goswami, R. N. Zare, F. Bouakline, and S. C. Althorpe, Phys. Chem. Chem. Phys. **13**, 8175 (2011).
[22] K. Koszinowski, N. T. Goldberg, A. E. Pomerantz, and R. N. Zare, J. Chem. Phys. **125**, 133503 (2006).
[23] S. C. Althorpe, J. Chem. Phys. **114**, 1601 (2001).
[24] A. I. Boothroyd, W. J. Keogh, P. G. Martin, and M. R. Peterson, J. Chem. Phys. **104**, 7139 (1996).
[25] F. Bouakline, S. C. Althorpe, and D. Peláez Ruiz, J. Chem. Phys. **128**, 124322 (2008).
[26] N. E. Shafer, A. J. Orr-Ewing, W. R. Simpson, H. Xu, and R. N. Zare, Chem. Phys. Lett. **212**, 155 (1993).
[27] C. J. Eyles, M. Brouard, C.-H. Yang, J. Klos, F. J. Aoiz, A. Gijsbertsen, A. E. Wiskerke, and S. Stolte, Nat. Chem. **3**, 597 (2011).
[28] *Applied Regression Analysis*, edited by G. Casella (Springer-Verlag, New York, 1998), p. 21.
[29] Exceptions to this rule are the differential cross sections for HD(v', j' = 0,1), for which the agreement between theory and experiment is typically very poor; e.g., see Ref. 14. However, for $j' > 1$, the agreement between theory and experiment is usually excellent, until the onset of the disagreements between theory and experiment discussed in this article.
[30] S. J. Greaves, D. Murdock, E. Wrede, and S. C. Althorpe, J. Chem. Phys. **128**, 164306 (2008).
[31] S. J. Greaves, E. Wrede, N. T. Goldberg, J. Zhang, D. J. Miller, and R. N. Zare, Nature (London) **454**, 88 (2008).
[32] N. T. Goldberg, J. Zhang, K. Koszinowski, F. Bouakline, S. C. Althorpe, and R. N. Zare, Proc. Natl. Acad. Sci. U.S.A. **105**, 18194 (2008).
[33] D. Skouteris, J. F. Castillo, and D. E. Manolopoulos, Comput. Phys. Commun. **133**, 128 (2000).
[34] E. Wrede, L. Schnieder, K. H. Welge, F. J. Aoiz, L. Bañares, J. F. Castillo, B. Martinez-Haya, and V. J. Herrero, J. Chem. Phys. **110**, 9971 (1999).